

Automatic Transition of Ballbot from Statically Stable State to Dynamically Stable State

Anish K Mampetta

CMU-RI-TR-01-00

August 2006

Robotics Institute
Carnegie Mellon University
Pittsburgh, Pennsylvania 15213

© Carnegie Mellon University

*Submitted in partial fulfillment of the requirements for the degree of
Master of Science*

Abstract

Dynamically stable mobile robots with a high centre of gravity and a small foot print are breaking new grounds in the field of mobile robotics. While in operation, these robots are dynamically stable, relying on inertial forces to maintain pose. And when not in operation, they rely on legs or kick stands to maintain static stability. The transition between the dynamic and static state should be automatic and smooth so as to give these robots truly autonomous capabilities. Ballbot has three retractable legs arranged in tripod configuration. Each leg is a servo controlled four bar slider crank mechanism with 1 DOF. In this work we explore means of automatic transition in Ballbot, by taking advantage of the properties of the leg mechanism. We consider two such methods, *lean and take-off*, and *simultaneous withdrawal*. We come up with generalized design intent for designing leg mechanisms to be used in dynamically stable robots. We also present the kinematic analysis of the spatial mechanism formed when the body and legs are taken together as a single mechanism.

Acknowledgement

I would like to thank my advisor Prof. Ralph Hollis for his invaluable guidance, help and support in pursuing this work. Many thanks to Dr. George Kantor, for helping out with various technical and software related aspects of Ballbot. It was really a pleasure working with Eric Schearer, thanks to you. Tom Lauwers's support in understanding the existing software and implementing new software is greatly acknowledged and thanked for. Last but not the least, I would like to thank members of my masters committee, Dr. Matthew Mason and Jonathan W Hurst, for lending time and will to evaluate this work. This work was supported in part by NSF grant IIS-0308067.

Contents

1	Introduction	1
2	Possible Methods of Transition	1
3	Stabilizing Feedback Controller	2
4	A closer look at the leg mechanism	4
4.1	Design Intent	5
4.2	Leg as an independent mechanism	6
5	Leg and body together as a Spatial Mechanism	9
5.1	Mobility Analysis	9
5.2	Kinematic Considerations	12
6	Revisiting transition modes	13
6.1	Lean and Take-off	13
6.2	Simultaneous withdrawal	16
7	Reverse Transition	17
8	Conclusion	18
9	Appendix	20
9.1	Relevant dimensions and calculations	20
9.2	Software Implemented	20
9.3	Hardware Modifications	21

1 Introduction

Dynamically stable mobile robots with a high centre of gravity and a small foot print are breaking new grounds in the field of mobile robotics. Tall robots intended for seamless interaction with humans necessitate wide base to maintain static stability, e.g., Xavier[6], Minerva[7], Nursebot[8], Rome-Juliet[9]. The wide base gives a low aspect ratio making constrained spaces like door ways inaccessible to the robot. Ballbot, introduced in [1], is a revolutionary new approach based on a single spherical wheel to take mobile robots to a new level of mobility and aspect ratio¹. Ballbot and other dynamically stable mobile robots [4], [5] are a paradigm shift compared to conventional statically stable systems. [1] discusses the details of the controller used to control Ballbot and presents preliminary results on station keeping and trajectory tracking.

Ballbot is a self contained dynamically stable mobility platform designed to be used in mobile robots intended to interact with humans. It has two states as far as stability is concerned: 1) the Dynamically Stable State (DSS), where the robot is actively balancing using a feed back controller and 2) the Statically Stable State (SSS), where the robot is not required to actively balance. In DSS, the only point of contact of the robot with the ground is the ball, and hence relies on inertial forces to maintain pose. Where as in the SSS the robot is resting on the legs arranged in tripod configuration. Motion is possible in both modes. In DSS the Ballbot moves around by balancing on the ball and orienting the body in the desired direction of motion. Where as in the SSS, the robot moves with legs sliding on the ground. Motion in the SSS is limited to smooth planar surfaces.

In order to give true autonomous capability to Ballbot, it is desirable to have automatic transition between the two states. This is however not an easy problem considering the physical limitations of the robot. The object of this work is to explore suitable strategy to make this transition and analyze the various aspects affecting this transition. Two aspects are particularly important while analyzing this problem: 1) the controller used during the transition and 2) the kinematic capability of the legs. Both aspects are looked into in this work. A controller that is meant to be operated dedicatedly during the transition phase is developed. The analysis of the legs is more of a reverse engineering process since the legs were already present on the bot while executing this work.

2 Possible Methods of Transition

The challenge is to withdraw the legs used in the SSS and smoothly transit into the DSS. During the retraction procedure, there are disturbances in the system that can cause the system to squirm and bring back the legs to sudden and undesirable contact with the ground causing impact loading on the system, possibly making the bot unstable. The problem of automatic transition from SSS to DSS in a dynamically stable system is a general and broader problem in the sense that it is faced by all dynamically

¹Aspect ratio is defined as the ratio of height to wheelbase. The approximate aspect ratios of various mobile robots designed for human robot interaction are, Ballbot(5.7), Xavier(2.1), Nursebot(2.2), Minerva(2.3), Romeo-Juliet(2.3)

stable mobile systems. For example, an aircraft overcomes this problem by creating enough momentum to make it robust to disturbances induced during the transition. A helicopter on the other hand creates enough upward thrust to make it robust during take-off. Ballbot neither can create enough momentum before take-off nor any upward thrust.

Our aim is to come up with a reliable and robust method for automatic transition that can be applied not only to Ballbot but also to a broad range of dynamically stable mobile robotic systems. The problem can be split into two, the “*take-off*” problem where the aim is transition from SSS to DSS and the “*landing*” problem, where the effort is to transit from DSS to SSS. We are considering two possible methods for the take-off problem,

1. Simultaneous Withdrawal, refers to take-off in which all three legs are withdrawn simultaneously. The balancing controller is turned on in tandem with the leg retraction or after a small delay.
2. Lean and Take-off, refers to take-off in which the body leans on two legs to create a known initial condition (angle) and take advantage of the response of the balancing controller to accomplish the transition.

Before going into the details of the various transition modes, we present the details of the controller used and analyze the capabilities of the existing leg mechanism.

3 Stabilizing Feedback Controller

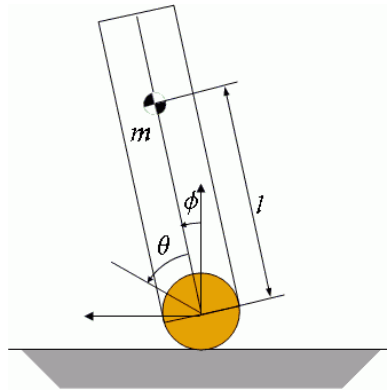


Figure 1: Ballbot frame assignment. ϕ represents the tilt of the body and θ represents the angular displacement of the ball. m is the lumped mass of the system and l is the height of CG from the center of the ball

For the purpose of developing a stabilizing controller, the simplified 2D model of the Ballbot is used [1]. The frame assignment for the model is shown in Figure 1. The purpose of the stabilizing controller is two fold: 1) Maintain the pose of the body upright vertical, referred to as *balancing* and 2) Maintain the position of the Ballbot, referred to as *station keeping*. The LQR based stabilizing controller used to control Ballbot is described in [1]. This is a velocity based controller that makes the Ballbot track a desired velocity.

During the automatic transition mode of lean and take-off, the initial angle of the body from the vertical is between 4 and 7 degrees. It was observed that when the initial angle of the body is large, the current version of the LQR controller on the Ballbot

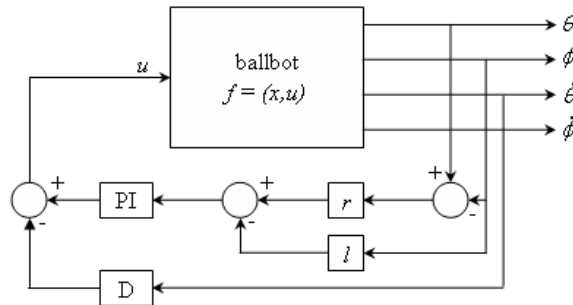


Figure 2: Block diagram of the balancing controller. r and l represents the radius of the ball and the height of the CG from the ground respectively

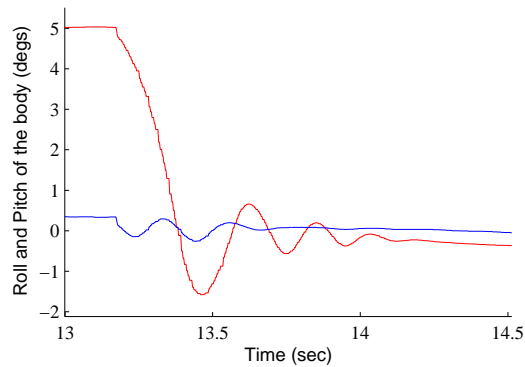


Figure 3: Response of the controller to an initial release angle of, pitch = 5 degree and roll = 0.3 degree. The controller was turned on at approx 13.2 seconds. The settling time is about 1 sec

was not able to balance the robot. For this reason, a dedicated controller that can be used during the transition phase is developed. This controller is a position based PID controller, which tries to move the ball to the point on the ground where the CG of the body passes through. Figure 2, shows the structure of this controller. The controller tries to maintain *balance*, totally ignoring the aspect of *station keeping*. The controller is quite robust to initial release angle. The response of the controller to an initial release angle is shown in Figure 3. This controller will be used during the transition phase and once the transition is complete, the controller will be switched to the stabilizing LQR controller, which can maintain balance as well as station.

4 A closer look at the leg mechanism

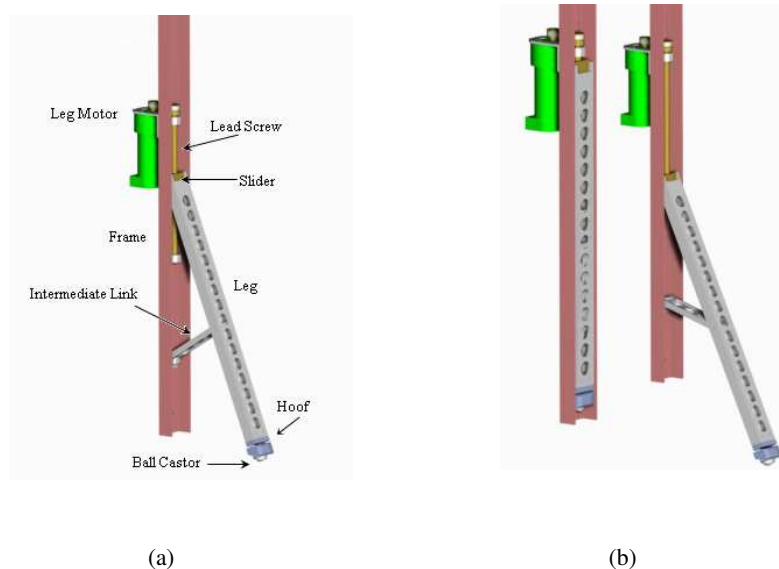


Figure 4: Snapshots of the leg mechanism. (a) Various components of the leg mechanisms (b) Legs completely retracted, and completely deployed

The Ballbot consists of a number of reconfigurable circular decks held together by three body length aluminum C section channels. These aluminum channels form the frame of the structure. There is one leg per frame. Figure 4 shows the snapshots of the leg mechanism. Figure 5 shows the spatial configuration of the legs. Each leg is approximately 48 cm long and made of standard aluminum channel. The legs are driven by a linear worm drive with a drive ratio of 0.16 cm/revolution of the drive motor. The tip of the leg, called the hoof, carries a limit switch and a ball castor. A spring and linear guide are incorporated between the legs and the hoof to add some compliance.

4.1 Design Intent

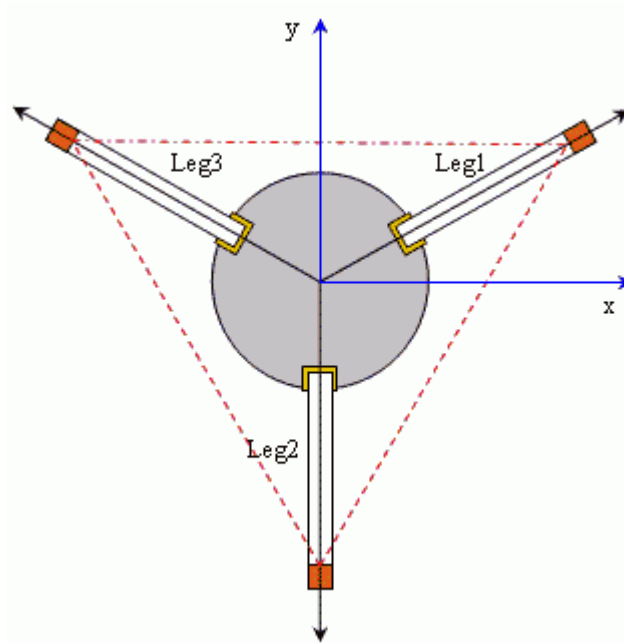


Figure 5: Top view of the Ballbot with all three legs deployed. The red triangle shows the convex polygon formed by the three legs. The CG of the robot should be within this triangle to maintain static stability

The design intent for the legs are as follows,

1. The legs should not be reverse drivable: In the statically stable state the robot should be able to maintain integrity of pose even when power is cut off. This requires that the legs should be non reverse drivable. In Ballbot, the legs are driven by a linear worm drive which satisfies this criterion.
2. The legs should move fast: It would be ideal to have a leg mechanism that retracts and deploys instantly. However, there is a compromise between the speed of the legs and the reverse drivability. A higher rate increases the reverse drivability and hence is non ideal.
3. The legs should be strong enough to carry the weight of the robot even when robot is resting in an off vertical position. In an off vertical pose, the weight of

the body is shared between two legs and the ball. The legs should be designed to maintain structural integrity in this position.

4. The mechanism should not have state of singularity in the range of operation. At points of singularity, the mechanical advantage of the mechanism tends to zero, arresting the motion of the legs.
5. The motion of the leg should be contained within the outer envelop of the body. In the case of Ballbot, the outer envelop is the polygon formed by the lines joining the legs (the red triangle in Figure 5).
6. The velocity of the hoof should be predominantly vertical and high at the lower extreme. Lower extreme refers to the point where the leg is completely deployed. This criteria implies that the hoof move away from the ground as fast as possible when the legs are retracted.
7. The approach velocity of the hoof should be small and smooth at the upper extreme. The upper extreme refers to the point where the leg is completely retracted into the body. This criterion makes sure that the legs sink into the frame smoothly.
8. The sliding friction between the hoof and the ground should be minimal so as to allow operation of the robot in the statically stable state. The robot can maneuver in the statically stable state by moving with the legs deployed. The legs slide on the ground in this mode of operation.

4.2 Leg as an independent mechanism

Considering each leg as an independent four bar linkage with the main frame as the fixed link gives us the freedom to analyze the motion of the leg independent of the whole system. Figure 6(a) shows the kinematic diagram of the mechanism. Figure 6(b) shows the coupler curve for the hoof. It can be seen from the coupler curve that the path traced by the hoof violates design intent 5. Motion of the leg is not entirely contained within the outer envelop of the robot. This is not a desirable characteristic because if the robot is standing close to a wall, the legs can intersect with the wall and cause a disturbing force on the system. The leg moves out of the envelop by about 1 cm. Hence the legs should be off by this distance from walls or obstacles when legs are operated.

Figure 7 shows the velocity profile of the hoof when the leg is withdrawn at constant speed (maximum speed of the leg motor, approximately 13 rps). It can be seen from Figure 7(b), that the velocity of the hoof at the lower extreme high, satisfying design intent 6. However the design intent 7, that the approach velocity should be small, is violated (fig.7(a)). It can be seen from the figure that the velocity in the x direction tends to infinity when leg approached the frame. This is because the mechanism tends to a state of singularity at this point. And for this reason, it violates the design intent 5 as well. A mechanically less elegant but a practical solution to this problem would be to modify the proportional gains P in the servo controller used to control the legs. In the case of Ballbot, the proportional gain is set as a linear function of the leg position as show in the equation (1).

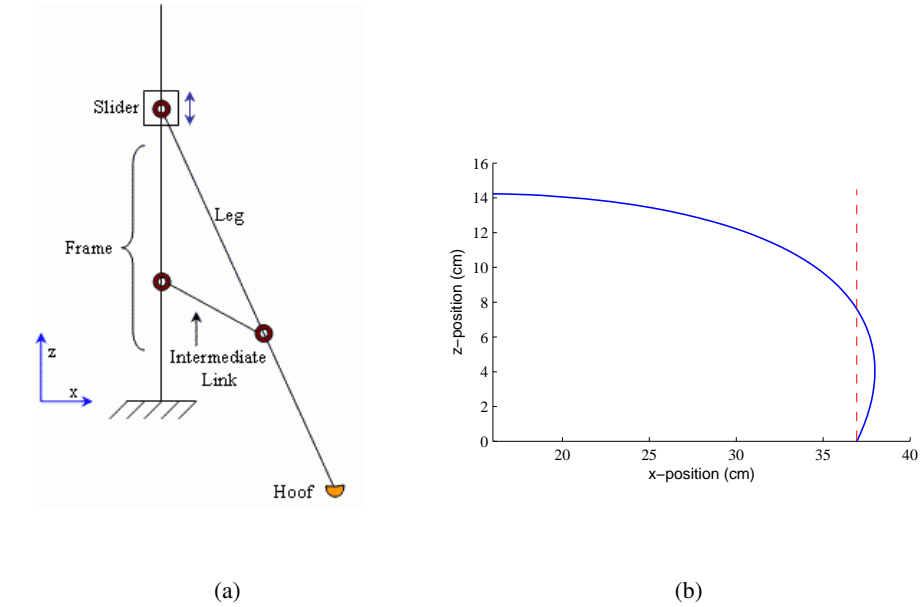


Figure 6: (a) The slider crank mechanism formed when the frame is considered to be fixed. The origin is set at the center of the ball (b) The curve shows the path traced by the hoof when the leg is retracted. The dotted vertical line denotes the outer envelop of the robot. It can be seen that during retraction, the legs go out of the envelop by approximately 1cm

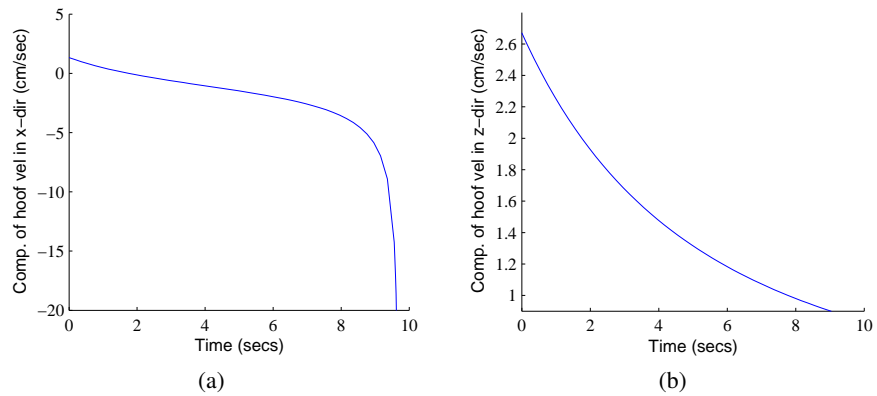


Figure 7: Velocity profile of the hoof when the legs are retracted from a completely deployed position. The time taken for full retraction is approximately 9 seconds (a) shows the profile of velocity in x-direction and (b) velocity in z-direction

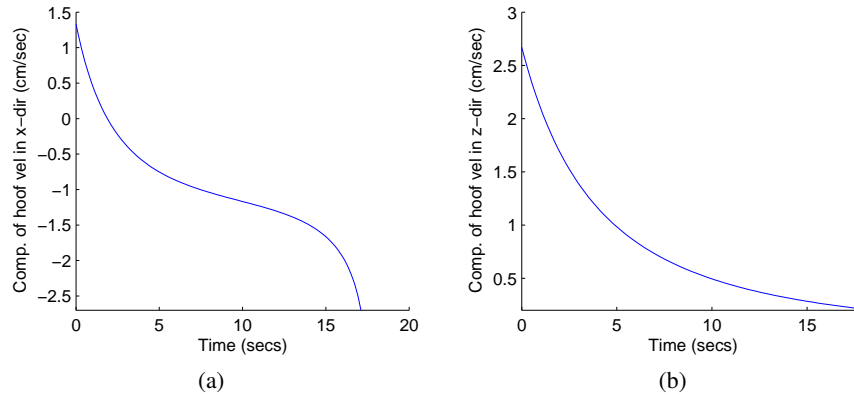


Figure 8: Modified velocity profile of the hoof. (a) shows the profile of velocity in x-direction and (b) velocity in z-direction

$$P = a + b\alpha \quad (1)$$

where, α denotes the position of the leg in terms of the number of revolutions of the leg motor to reach the particular position from a completely retracted state. α varies from 0 (completely retracted) to 110 (completely deployed). Figure 9 shows the actual controller implemented on ballbot. The resulting velocity profiles are shown in Figure 8. This modification helps to satisfy the velocity criteria, but the singularity cannot be eliminated without redesigning the mechanism. At the singularity, the mechanical advantage of the system approaches zero, demanding very large torque to initiate mo-

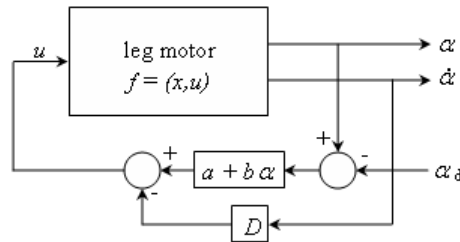


Figure 9: Block diagram of the servo controller on leg motors. α denotes the position of the leg in terms of the number of revolutions of the leg motor to reach the particular position from a completely retracted state. α varies from 0 (completely retracted) to 110 (completely deployed). α_d denotes the desired position of the leg.

tion. In the case of Ballbot, the leg mechanism is only close to singularity (and not at a singularity) at the completely retracted position, hence the legs are able to come out of it with reasonable torque.

5 Leg and body together as a Spatial Mechanism

In the mode of lean and take-off, the body leans on two legs. During this state, the body and the two active legs form a parallel spatial mechanism with 2 degrees of freedom. The input to the mechanism is the position of the base of the legs (joints J5 and J6 in fig.10). The output of the mechanism is the orientation of the body, defined by the pitch and roll of the body. Mobility analysis of the system gives a deeper perspective of the mechanism. For the purpose of analysis, any given joint in the mechanism is considered as combinations of 1 dof revolute(R) and prismatic (P) pairs.

5.1 Mobility Analysis

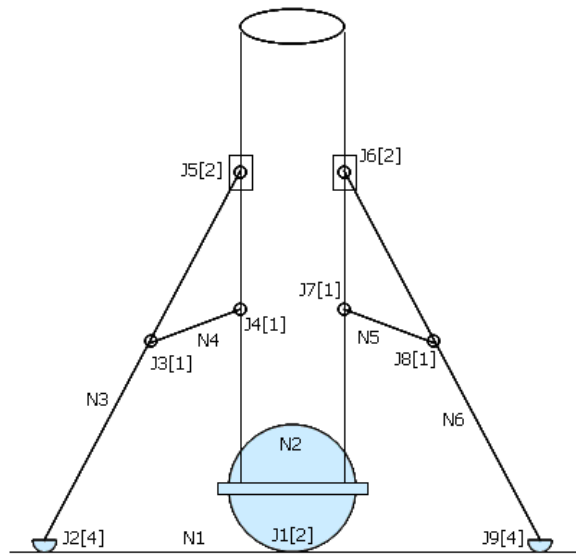


Figure 10: Kinematic model of the spatial mechanism formed when Ballbot leans on two legs. J represents a joint and N represents a link. The number inside the square parenthesis shows the dof's at the particular joint.

Mobility of this mechanism can be analyzed using the 3D form of the Kutzbach mobility criteria [2], give as

$$m = 6(n - 1) - 5j_1 - 4j_2 - 3j_3 - 2j_4 - j_5 \quad (2)$$

where m represent the mobility, n is the number of links in the mechanism and j_i is the number of joints with i dofs. In Figure 10, J represents the joints and the DOF of the particular joint is denoted in square parenthesis. J5 and J6 are PR joint [2 dofs], the position of which are controlled by the leg motors, hence they form the input to the mechanism. J2 and J9 are RRPP joint [4 dof]. J1 is the joint formed between the ball and the ground, this joint is RR. N represents the links in the mechanism, N1 represents the ground and N2 represent the body and the ball². By observation, $n = 6, j_1 = 4, j_2 = 3, j_3 = 0, j_4 = 2, j_5 = 0$. The mobility of the mechanism is therefore,

²It is assumed that there is no relative motion between the body and the ball during leaning, hence they are considered as a single link.

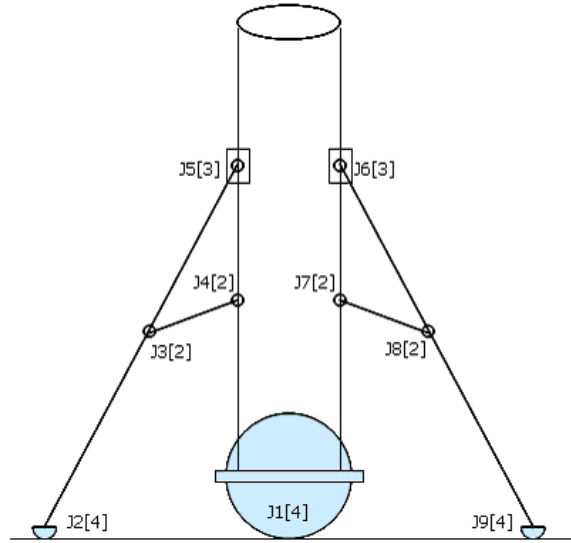


Figure 11: Kinematic model of Ballbot with additional dof's

$$m = 6(6 - 1) - 5 * 4 - 4 * 3 - 2 * 2 = -6, \quad (3)$$

which is not equal to 2 as supposed to be. This is because the Kutzbach criterion³ gives a negative value for mobility of the mechanism when there are redundant constraints in the mechanism [2]. Even though this does not affect the kinematics of the system, while analyzing the forces in the mechanism we will encounter problems because the redundant constraints determine how the forces will be shared when the motion freedom is eliminated. Thus the static force analysis problem becomes over constrained and there exists statically indeterminate forces. We can also see that the number of indeterminate forces will be equal to the magnitude of mobility predicted by the Kutzbach criteria above.

The redundant constraints exist because we are restricting each leg to move in a plane by using single degree of freedom revolute joints (at J3,J4,J7,J8 and the R joints on J5 and J6). The redundant constraints can be identified by observation⁴. These constraints can be eliminated by adding additional degrees of freedom at these points. Figure 11, shows the joints with extra degrees of freedom. In this case $j_1 = 0, j_2 = 4, j_3 = 2, j_4 = 3, j_5 = 0$, and the corresponding mobility is,

$$m = 6(6 - 1) - 4 * 4 - 3 * 3 - 2 * 3 = 2, \quad (4)$$

which is in accord with the observed mobility.

The mobility analysis reveals a fundamental limitation in this kind of leg mechanism as far as leaning on two legs is concerned. Even though the individual legs are appropriately designed to serve the design intend specified in section 4.1, when the legs combine with the body to form a spatial mechanism, the reaction forces in the joints cannot be determined, hence making it impossible to analytically design the joints in terms of calculating the bearing of the pins and sliders that form the joints.

We can also see that the motion of the leg is not contained in a single plane when the legs operate as a part of the spatial mechanism. Figure 12, shows the path traced by the hoof when the body leans on two legs. The straight line at a slope of 30 degrees indicated the ideal trajectory traced by the hoof on the ground if the motion of the leg is contained in a single plane. The curved line shows the actual path traced by the leg. It is evident from the figure that the legs move out of the plane and such out of the plane motion imposes additional bending moments on the joints. Moreover, the magnitude of the bending moment in individual joints cannot be statically determined. Hence, while designing the pins (joints), we are forced to resort to empirical methods to accommodate these statically indeterminate forces and moments. To get away with these effects, it is a common design practice to incorporate some form of compliance in the joints, in the form of soft bushes. These compliant bushes absorb unaccounted strains hence making sure that the pins are not over stressed.

³The Kutzbach criteria predicts a lower limit on the mobility criteria.

⁴Two constraints to maintain J3,J4,J5 parallel. Two constraints to maintain J6,J7,J8 parallel. Two constraints that prevents the translation of J1. Total of 6 redundant constraints, which is equal to the magnitude of mobility predicted by Kutzbach criteria.

5.2 Kinematic Considerations

Since the body and two active legs form a spatial mechanism and since we exploit this mechanism to orient the body, it is reasonable to expect to have some transformation that relates the orientation of the body p , defined in terms of pitch ϕ_1 and roll ϕ_2 of the body to the position of the legs, in the form of

$$p(\phi_1, \phi_2) = T * f(\alpha_1, \alpha_2) \quad (5)$$

However, because of the nature of the constraints at some of the joints, such a relationship is not possible. For instance, joints J2, J1 and J9 (fig. 10) are not hard constraints. We know that the mobility of the spatial mechanism, $m = 2$, and the number of links in the mechanism, $n = 6$. We can substitute the values of m and n in equation (2) to get the following relationship.

$$5j_1 + 4j_2 + 3j_3 + 2j_4 + j_5 = 28 \quad (6)$$

All possible combinations of j_i 's satisfying the equation (6) gives the same mobility to the mechanism. And in general, the behavior of joints depends on the constraint

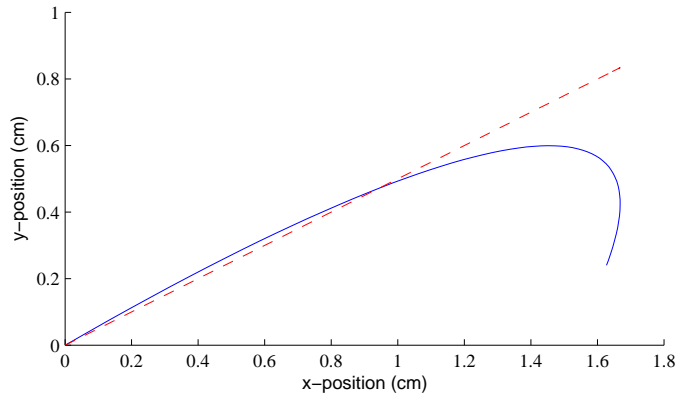


Figure 12: Path traced by the hoof on the ground when the body is leaning on two legs. The curved line shows the actual path traced. The straight line shows the path the hoof would trace if the legs are not deflected out of plane.

forces, friction at the contact and the compliance at the joints. Hence the relative motion is non deterministic.

However, if we limit the motion of the system to some special cases and assume that the contact friction between the legs and the ground is uniform, we can have a one to one relationship between the tilt of the body and the position of the leg. One such special case is where both the active legs are retracted by same amount simultaneously. In this particular case, the lean of the body is confined to the plane bisecting the two legs (the yz plane, refer fig5). Figure 13 shows this relationship. And the second order polynomial equation that fits this curve with a norm of 0.6956 is

$$\phi = -0.0027 + 0.5856 * (110 - \alpha) + 0.2334 * (110 - \alpha)^2 \quad (7)$$

where α represents the number of revolutions of the leg drive motors measured from completely retracted position and ϕ represents the tilt of the body in degrees along the plane bisecting the two active legs.

6 Revisiting transition modes

In the light of the analysis presented on the leg mechanism, we can revisit the transition modes for a more in depth analysis.

6.1 Lean and Take-off

In the *lean and take-off* mode the body is made to lean on two legs. The third leg then loses contact with the ground and can be completely retracted. The lean of the body

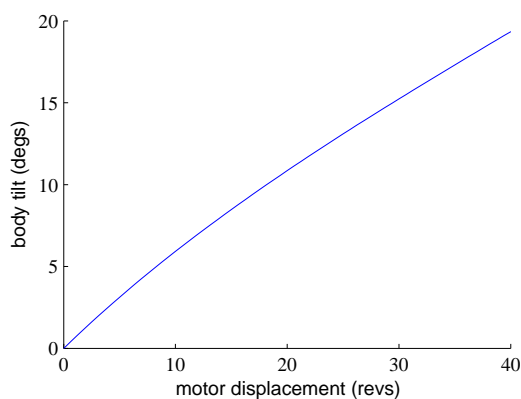


Figure 13: Body tilt vs leg position. Leg position is specified in terms of no. of revolutions of the leg motor. Body tilt is measured in the plane bisecting the plane of the legs

can be adjusted by controlling the position of the two active legs. Equation 7, gives the relationship between the lean of the legs and orientation of the body. When the controller is turned on, the ball moves in the direction of the lean pushing the body in the opposite direction, taking the active legs off the ground. The response of the body to an initial lean angles is presented in Figure 3. We can parameterize the position of the leg with the lean angle of the body to get a lower limit on the leg position of the active legs. The parametric curve is shown in the Figure 14. The lean and the position of the legs should be outside the shaded area throughout the transition process.

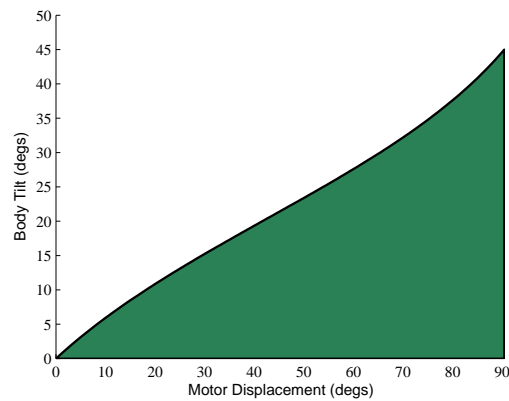


Figure 14: Parameterization of body tilt with leg position

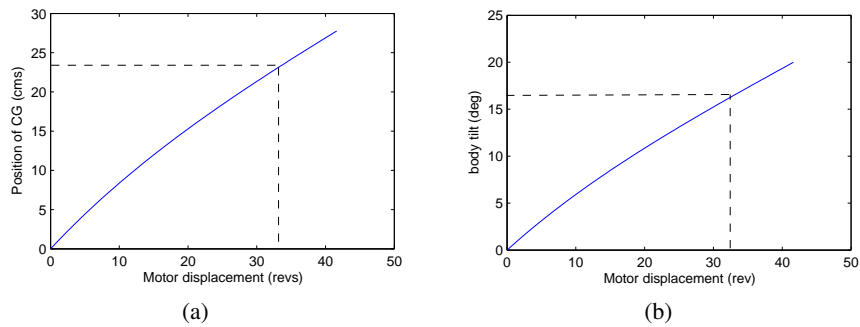


Figure 15: (a) Position of the Center of Gravity (CG) for various leg positions, (b) lean angle of the body for various leg positions

It is also required to find out the limit of the lean angle. There are two factors that limit the lean angle of the body, and they are -

- a. The centre of gravity (CG) of the body should be within the convex hull formed by the active legs and the ball to ensure static stability. The red triangle in Fig-

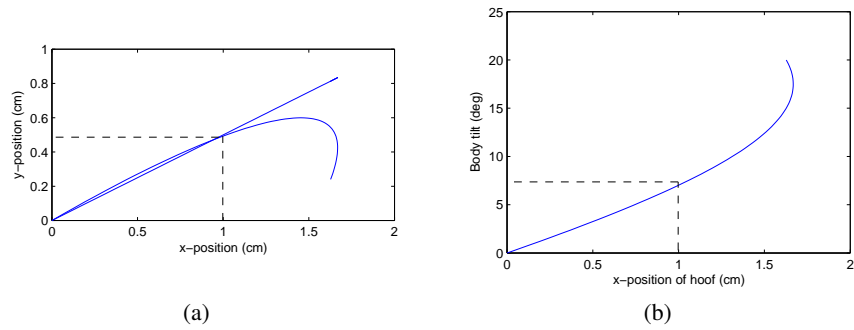


Figure 16: (a) Path traced by the hoof on the ground when the body leans on two legs, (b) lean angle of the body Vs the x position of the hoof.

Figure 17 shows the convex hull. From geometric calculation, the maximum distance the CG can travel within the convex hull, from the center of the ball, is approximately 23.2 cm.⁵ Figure 15(a), shows the distance traveled by the CG from the centre of the ball when the legs are retracted. Comparing this with Figure 15(b), we can deduce that the limit of travel of the CG is reached when the

⁵Refer Appendix for more details.

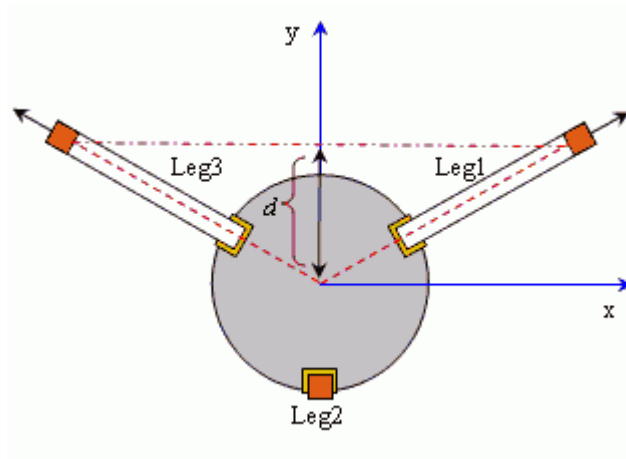


Figure 17: Top view of the robot with one leg completely retracted. The red triangle shows the convex polygon formed between the two active legs and the ball. d represents the maximum distance the CG can travel. In the case of Ballbot $d = 23.2\text{cm}$

body is leaning at 16 degrees from the vertical.

- b. The lean angle should be within the kinematic limits of the leg mechanism. In Figure 16(a), the curved trajectory represents the actual path traced by the hoof on the ground (xy plane) when the body leans on two legs and the straight line represents the ideal path the hoof should take so that the mechanism remains within the plane it is designed to operate. And Figure 16(b), represents the lean angle of the body with the planar x displacement of the hoof. Comparing these plots, we can infer that the kinematic limit of the spatial mechanism is reached when the body is leaning at an angle of 7 degrees from the vertical.

Hence we can conclude that the present design of Ballbot allows it to lean by an angle of 7 degrees without straining the leg mechanism⁶. Hence, in the lean and take-off mode, the lean angle should be less than 7 degrees. The sequence of operation for doing lean and take-off is listed below.

1. Bring the body to upright, statically stable configuration by completely extending all the legs.
2. Set the body to take-off configuration: Lean on any two legs in the range of 0-7 degrees. Withdraw the third leg completely (or partially).
3. Turn on the balancing controller (or take-off controller if there is a dedicated take-off controller as in case of Ballbot).
4. Withdraw all the legs completely.
5. Switch to the stabilizing controller: Once take-off is complete, switch to stabilizing (balancing and station keeping) controller.

6.2 Simultaneous withdrawal

In this mode, all the legs are withdrawn simultaneously and the balancing controller is turned on in tandem with the leg withdrawal. There may or may not be a delay in turning on the controller, depending up on the system. In Ballbot, we turn on the balancing controller in tandem with the withdrawal of legs. This approach works, but the disadvantage is that we do not have direct control on the direction of take-off nor can quantify the capacity of the bot to reject disturbance during take-off. In the case of lean and take-off, the torque driving the ball is proportional to the lean angle and in the direction of the lean. This is because the initial response of the take-off controller is directly proportional to the lean angle. By having a large enough lean angle, we can generate sufficiently high response in the desired direction to reject disturbances occurring during the take-off. This is not possible in case of simultaneous withdrawal because the lean angles are small and the lean direction is random. A possible way to get around this problem would be to come up with a controller that is immune to initial disturbances. This is a possibility that has to be explored in future work.

⁶This feature should be incorporated as a design intent, so that this is taken care of in the design process.

Another issue with simultaneous withdrawal is that the initial position of the legs are not controlled, hence this method gives no guarantee that the lower limit of the leg position (fig. 14) is satisfied under all circumstances. In spite of all these limitations and lack of elegance, this approach works quite well in the case of Ballbot. One major advantage of this method is that we might be able to get away from having a dedicated take-off controller.

7 Reverse Transition

The reverse transition or *landing* refers to the transit from Dynamically Stable State to a Statically Stable State, is equally challenging. Especially so because we cannot exploit the leg mechanism as the legs are not in contact with the ground. In Ballbot, during the reverse transition phase, all three legs are deployed simultaneously within the range of statically stable state of the robot and then the balancing controller is switched off. The body falls on any two legs, depending upon the orientation of the body at the instant the controller is turned off and goes to statically stable but off vertical pose. The maximum height of the legs from the ground during the transition from DSS to SSS should be such that the lean angle of the body should be within the allowable lean of the body in the SSS. In the case of Ballbot this limit is 7 degrees and from Figure 14 we can calculate the corresponding position of the leg.

The body can be brought back to upright vertical pose from the off vertical pose by completely extending all the three legs simultaneously. In a more general setting, if the legs are designed to be operated as part of the spatial mechanism thus formed and if the friction between the legs and the ground are assumed to be uniform, a inverse kinematic relationship between the orientation of the body and the position of the legs exists and can be used for fine control of the body orientation in the statically stable phase of reverse transition. But as we have seen in section 5.2, such a relationship is not feasible in the case of Ballbot.

Once the body is brought back to the upright position, it might not be at the desired location. This is because, 1) The position of the robot cannot be controlled once the controller is turned off, 2) The controller used during reverse transition may not do station keeping. We can bring back the robot to the desired final position by driving the robot in statically stable state once the transition is complete. This is possible because each hoof carries a ball castor. The steel ball in the ball castor forms a point contact with the ground with low sliding friction. The bot can be driven around on a plane surface by operating the drive mechanism in the statically stable state. In such a mode, Ballbot is like any other statically stable mobile robot except that it is driven by a spherical wheel. The position of the bot can be controlled by using a simple PID controller. However, care has to be taken to make sure that the body does not accelerate or decelerate at a rate that pushes the resultant of acceleration of the body and gravity vector outside the convex polygon formed by the three legs. Under these circumstances, the bot can become unstable and tip over.

In the case of Ballbot, the sequence of operation undertaken during reverse transition is enumerated below,

1. Switch from the general controller to reverse transition controller. The reverse transition controller is same as the take-off controller.
2. Deploy the three legs simultaneously within the range of statically stable state of the robot.
3. Turn off the reverse transition controller and let the robot statically balance on two legs and the ball.
4. Reorient the bot to upright vertical pose by completely extending all three legs.
5. Reposition the bot to the required final position by moving the bot in statically stable state.

8 Conclusion

By exploiting the properties of leg mechanisms in a dynamically stable mobile robots, it is possible to accomplish automatic transition from static to dynamic state through the process of *lean and take-off*. A generalized framework for designing legs so as to incorporate this capability is derived. It is possible to orient the robot by operating the legs and body as a single spatial mechanism. Kinematic analysis of the spatial mechanism reveals the limitation of legs when they are multitasked for transition. These limitations can be overcome by designing the legs to accommodate the capability of automatic transition. It is desirable to use a dedicated controller, immune to large deviation from vertical during the transition phase to accommodate for the disturbances encountered during the process. It is also possible to accomplish transition simply by withdrawing the legs simultaneously, referred to as *simultaneous withdrawal*. However, in this process we have much less control over the body during the transition. During the reverse transition, legs are not used until after transition to static state. Once the static state is obtained by letting the body fall on the legs, leg position is controlled to reorient the body. With the legs deployed, a dynamically stable robot can be operated in a statically stable mode to reposition the robot to the desired final location.

Reference:

1. T.B Lauwers, G.A Kantor and R.L Hollis, A Dynamically Stable Single-Wheeled Mobile Robot with Inverse Mouse-Ball Drive, Proc, IEEE Intl Conf. on Robotics and Automation, Orlando, FL, May 15-19, 2006
2. Theory of Machines and Mechanisms, Joseph Edward Shigley, John Joseph Uicker, McGraw-Hill, Inc. 1995
3. Mechanics of Robotic Manipulation, Matthew T Mason, MIT Press, Cambridge, MA, 2001

4. Hoa G. Nguyen, Greg Kogut, et al., A Segway RMP-based robotic transport system, SPIE Proc. 5609: Mobile Robots XVII, Philadelphia, PA, October 27-28, 2004
5. Segway Robotic Mobility Platform (RMP), <http://www.segway.com/products/rmp/>
6. R. Simmons, J. Fernandez, R. Goodwin, S. Koenig, and Joseph OSullivan. Xavier: An autonomous mobile robot on the web. Robotics and Automation Magazine, 1999.
7. S. Thrun, M. Bennewitz, W. Burgard, A.B. Cremers, Frank Dellaert, Dieter Fox, D. Haehnel, Chuck Rosenberg, Nicholas Roy, Jamieson Schulte, and D. Schulz. MINERVA: A second generation mobile tourguide robot. In Proc. of the IEEE Intl Conf. on Robotics and Automation (ICRA99), 1999.
8. G. Baltus, D. Fox, F. Gemperle, J. Goetz, T. Hirsch, D. Magaritis, M. Montemerlo, J. Pineau, N. Roy, J. Schulte, and S. Thrun. Towards personal service robots for the elderly. In Proc. Workshop on Interactive Robotics and Entertainment (WIRE), Pittsburgh, PA, 2000.
9. O. Khatib, K. Yokoi, K. Chang, D. Ruspini, R. Holmberg, and A. Casal. Vehicle/arm coordination and multiple mobile manipulator decentralized cooperation. In Proc. of the IEEE/RSJ Intl Conf. on Intelligent Robots and Systems, pages 546553, Osaka, 1996.

9 Appendix

9.1 Relevant dimensions and calculations

Some of the relevant dimensions of Ballbot are given below. The dimensions are measured from the physical system and are only approximate. For exact dimensions refer the latest CAD model of the robot.

1. Calculation of drive ratio of the leg drive: Pitch of the lead screw = 1/16" (Standard 3/8" Withworth Screw) Drive ratio = $2.54/16$ cm/rev = 0.16 cm/revs
2. Stroke of the leg drive = 9" = 22.8cm
3. Length of the legs = 19" = 48.2cm
4. Size of the equilateral triangle formed by the three legs = 26" = 66cm
5. Radius of the circle enclosing this triangle = 44 cm
6. Size of the convex polygon (which is a triangle)formed by two active legs and the ball is = 66x44x44cm
7. Theoretical distance by which the CG can move before it moves out of the convex polygon = 29.1 cm.
8. Practical limit, 80 percentage of theoretical limit = 23.2cm.
9. Height of CG from the ground (as on Aug 18,2006) = 32" = 81.2cm

9.2 Software Implemented

1. legs-move.c: servo control for the position of the legs. The program reads in the desired position of the leg in terms of leg motor revolutions and drives the legs to the desired position. The range of operation is 0-110 revolutions of the motor. An input of "0" retracts the legs completely and "110" deploys the legs completely. Legs can be controlled independently, any combination of two legs or all three legs simultaneously.
2. takeoff-leaning.c: executes the lean and take off maneuver. The program brings the body to upright position, then leans the body on legs 1 and 3, retracts the leg 2 and then balances the body by taking off from legs 1 and 3. Once the body is in balance, all three legs are retracted completely.
3. takeoff-simultaneous.c: executes the simultaneous withdrawal maneuver. The program brings the body to upright position, withdraws the legs simultaneously and turns on the balancing controller simultaneous. Once the body is in balance, all three legs are retracted completely.

The source code for the implementation is located at, /imu/crossbowInterface/src

9.3 Hardware Modifications

1. Addition of a second quadrature encoder IP to read in leg motor encoders: Ballbot was upgraded with an extra quadrature encoder IP card to read in the encoders on the leg motors. The card was added to the slot B on the second ATC-30 card. Necessary functions and header files to read in the encoder values are implemented. The include file, 'atc30.c', was made modified to define the base address of the new IP card.
2. Addition of limit switches on the legs: Limit switches were added to the tip of each leg. The switches are read in through the port 0 of the digital I/O IP. Software necessary to read in the switches are implemented.
3. Upgrading the leg motors: The existing leg motors did not have enough torque to retract the legs fast enough for automatic transition as well as it lacked encoders for closed loop control. These were replaced with higher capacity motor with integrated encoders. The specification of the new motor is as follows.

Make: Pittman, Product ID: GM9236S015-R1

24V, Gear Ratio: 5.9:1, Max Load: 1.24N-m, No-Load Speed: 834 rpm

Encoder: 500 cpr